symmetry

MDPI

Article

Ramsey Approach to Symmetry

Edward Bormashenko

Department of Chemical Engineering, Engineering Faculty, Ariel University, Ariel 407000, Israel; edward@ariel.ac.il

Abstract

Symmetry operations are usually studied within the frameworks of group theory, geometry, and operator algebra. In the present work, a Ramsey-theoretic approach to symmetry is developed. Symmetry operations are treated as operators serving as vertices of complete bi-colored graphs, called symmetry graphs (SGs). Two symmetry operators are connected by a maroon edge when they commute and by a teal edge when they do not commute. Thus, the commutation structure of a symmetry group is transformed into a combinatorial object suitable for Ramsey-theoretic analysis. The introduced coloring is generally non-transitive, leading naturally to nontrivial complete bi-colored graphs constrained simultaneously by group-theoretical and combinatorial principles. It is shown that every symmetry graph containing six vertices necessarily contains either a monochromatic commuting triangle or a monochromatic non-commuting triangle as a direct consequence of the classical Ramsey theorem $R(3,3) = 6$. The framework is illustrated for the symmetry groups of the equilateral triangle, regular tetrahedron, crystallographic point groups, infinite Cairo pentagonal tilings, and the triangular Ising ferromagnet. Higher-order structures, including teal quadrangles, second-order graph symmetries, infinite monochromatic cliques, and Lie-algebraic constraints arising from the Jacobi identity, are discussed. The proposed framework establishes a new connection between symmetry theory, Ramsey theory, graph theory, crystallography, and operator algebra.

Keywords: symmetry; operators; commutation; complete bi-colored graphs; Ramsey theory; Jacobi identity; tilings; Ising model

1. Introduction

Symmetry is one of the central organizing principles of mathematics, physics, chemistry, crystallography, and engineering. Symmetry groups describe the invariance of geometric objects under transformations such as rotations, reflections, translations, and inversions. The mathematical language of symmetry is group theory, where symmetry operations are represented by operators acting on an appropriate representation space [1–5]. The algebraic structure of symmetry groups plays a fundamental role in geometry, crystallography, quantum mechanics, molecular physics, and field theory [6–12].

An important aspect of symmetry groups is the commutation structure of symmetry operators. Certain symmetry operations commute and may therefore be simultaneously applied independently of order, whereas others do not commute, reflecting intrinsic structural incompatibilities within the symmetry group. Commutation relations are central in many branches of mathematics and physics, especially in quantum mechanics, Lie theory, representation theory, and crystallography [13–18]. Despite the extensive study of symmetry groups, the commutation structure of symmetry operators has rarely been treated from a combinatorial and Ramsey-theoretic viewpoint.

Check for updates

Academic Editor: Michel Planat

Received: 20 May 2026
Revised: 12 June 2026
Accepted: 14 June 2026
Published: 16 June 2026

Copyright: © 2026 by the author. Licensee MDPI, Basel, Switzerland. This article is an open access article distributed under the terms and conditions of the Creative Commons Attribution (CC BY) license.

The graph representation of the groups has been already intensively addressed [19–24]. The notion of the commuting graph was introduced by Brauer and Fowler in their seminal paper [19]. Let G be a finite group. The commuting graph of G is the graph with vertex set G in which two vertices x and y are joined if $xy = yx$. Brauer and Fowler demonstrated that only a finite amount of groups of even order can have a prescribed centralizer [19]. Commuting graphs were intensively studied [20–25]. In the classical commuting graph of a group, commuting pairs are represented by edges while non-commuting pairs are simply omitted. In contrast, the present work employs complete bi-colored graphs in which both commuting and non-commuting relations are represented explicitly as complementary edge colors. Thus, the introduced symmetry graphs belong naturally to the framework of Ramsey-type colorings rather than ordinary commuting graphs. The suggested framework does not merely reformulate commuting graphs in different notations; rather, it transforms the commutation structure of symmetry groups into a Ramsey-type combinatorial object in which unavoidable monochromatic substructures become mathematically meaningful. In this sense, non-commuting relations acquire the same structural status as commuting relations.

Ramsey theory studies unavoidable structures emerging in sufficiently large combinatorial systems [12,26–30]. The classical Ramsey theorem states that every complete graph whose edges are colored by two colors contains a monochromatic triangle provided the number of vertices is at least six: $R(3,3) = 6$. Ramsey-type methods have found applications in graph theory, logic, topology, combinatorics, computer science, and, more recently, in physical systems and operator structures [31–36]. In particular, Ramsey-theoretic approaches were recently applied to quantum-mechanical operator systems, where observables were represented as vertices of graphs [37–40].

In the present paper, we extend the Ramsey viewpoint to symmetry theory itself. Symmetry operations are regarded as operators forming vertices of a complete bi-colored graph [41–44]. Ramsey approach has been already applied for the analysis of symmetry [41]. We propose an alternative coloring scheme based on the commutation of symmetry operators, seen as the vertices of the complete, bi-colored graph. Two symmetry operators are connected by a maroon edge when they commute and by a teal edge when they do not commute [45]. The resulting graph is called the symmetry graph (SG). This construction transforms the algebraic commutation structure of a symmetry group into a combinatorial object suitable for Ramsey-theoretic analysis.

The introduced coloring is generally non-transitive. Indeed, commutation of operators is not sufficient to guarantee transitivity of the corresponding graph coloring, and non-commutation is also non-transitive in general. Consequently, symmetry graphs are highly nontrivial complete bi-colored graphs whose structure is constrained simultaneously by group-theoretical and Ramsey-theoretical principles.

The main purpose of the present work is to formulate the Ramsey approach to symmetry and to demonstrate that unavoidable monochromatic structures naturally emerge in symmetry groups. In particular, every symmetry graph containing six vertices necessarily contains either a monochromatic commuting triangle or a monochromatic non-commuting triangle. We show that these structures arise naturally even for simple geometric objects such as the equilateral triangle and regular pentagon. The proposed framework establishes a bridge between symmetry theory, graph theory, operator algebra, and Ramsey combinatorics.

The suggested approach is general and may be extended to finite and infinite symmetry groups, crystallographic groups, Lie groups, operator algebras, and quantum symmetries. In this sense, symmetry graphs may provide a new combinatorial language for the study of algebraic structures generated by symmetry operations. The novelty of the work lies in applying Ramsey-theoretic reasoning to symmetry-generated commutation structures

and in identifying physically meaningful monochromatic substructures associated with Abelian and non-Abelian sectors of symmetry groups.

The paper is organized as follows. Section 2 introduces the coloring procedure generating the bi-colored complete symmetry graph and formulates its basic properties. The notion of the symmetry graph is rigorously defined, and the non-transitive character of the induced coloring is discussed. The framework is then illustrated for several representative examples, including the equilateral triangle, regular tetrahedron, crystallographic point groups, infinite Cairo pentagonal tilings, and the triangular Ising ferromagnet. Finite and infinite Ramsey-type results for symmetry graphs are formulated and proved. One-dimensional structures generate semi-transitive graphs. Section 3 extends the developed approach to physical systems through the example of the Ising ferromagnet and motion of the particle in the central potential. Section 5 addresses the Lie-algebraic aspects of the framework and discusses constraints imposed by the Jacobi identity on commutation-closed symmetry graphs. Finally, the Discussion and Conclusions summarize the main results, physical interpretations, and possible future developments of the Ramsey approach to symmetry.

2. Results

2.1. Coloring Procedure Resulting in the Bi-Colored, Complete Graph

Consider the set $\mathfrak{H}$ of n symmetry operations related to a given geometric object. Every operation is represented by the symmetry operator $\mathfrak{H} = \{\hat{S}_1, \hat{S}_2, \ldots, \hat{S}_n\}$. Let us rigorously define the symmetry operators.

Definition 1. *Let X be a geometric object embedded in a space M (for example, the Euclidean plane or three-dimensional Euclidean space). A symmetry operation of X is a bijective transformation: $\hat{S} : M \to M$, such as $\hat{S}(X) = X$. The transformation $\hat{S}$ is called a symmetry operator of the object X. The set of all such operators forms the symmetry group $\mathfrak{H} = \{\hat{S}_1, \hat{S}_2, \ldots, \hat{S}_n\}$.*

The operators within our approach serve as the vertices of the bi-colored graph. Coloring of the edges of the graph is defined by commutation relations. Commutator is defined by Equation (1):

$$[\hat{S}_i, \hat{S}_j] = \hat{S}_i\hat{S}_j - \hat{S}_j\hat{S}_i. \quad (1)$$

The operators commute when Equation (2) takes place:

$$\hat{S}_i\hat{S}_j = \hat{S}_j\hat{S}_i;\ [\hat{S}_i, \hat{S}_j] = 0. \quad (2)$$

The commuting operators are connected within our approach by the maroon link/edge, whereas the non-commuting operators (i.e., $\hat{S}_i\hat{S}_j \neq \hat{S}_j\hat{S}_i$ is true) are connected by the teal edge, as depicted in Figure 1.



Figure 1. Coloring procedure resulting in the creation of the bi-colored, complete symmetry graph. (**A**) Operators $\hat{S}_i$ and $\hat{S}_j$ are commuting; they are connected by the maroon edge. (**B**) Operators $\hat{S}_k$ and $\hat{S}_l$ are non-commuting; they are connected by the teal link.

The introduced coloring procedure results in the bi-colored, complete, Ramsey-type graph which is called the "symmetry graph" and is abbreviated as SG in the text. Let us rigorously define the symmetry graph.

Definition 2. *Let $\mathfrak{H} = \{\hat{S}_1, \hat{S}_2, \ldots, \hat{S}_n\}$ be the set of symmetry operators of a geometric object X, where every operator $\hat{S}_i$ satisfies $\hat{S}_i(X) = X$. We construct the complete graph $SG = (V, E, c)$, called the symmetry graph, as follows: the vertex set is $V = \{\hat{S}_1, \hat{S}_2, \ldots, \hat{S}_n\}$. The edge set is $E = \{\{\hat{S}_i, \hat{S}_j\} : i \neq j\}$. The coloring function $c : E \to \{maroon, teal\}$ is defined by:*

$$c = (\hat{S}_i, \hat{S}_j) = \begin{Bmatrix} maroon, & if\ \hat{S}_i\hat{S}_j = \hat{S}_j\hat{S}_i \\ teal, & if\ \hat{S}_i\hat{S}_j \neq \hat{S}_j\hat{S}_i \end{Bmatrix}. \tag{3}$$

Thus, commuting symmetry operators are connected by maroon edges, whereas non-commuting symmetry operators are connected by teal edges. The symmetry graph is therefore a complete bi-colored graph encoding the commutation structure of the symmetry group associated with the geometric object.

Let us discuss the properties of the symmetry graph.

(i) The coloring of the symmetry Ramsey graph is not arbitrary. It is induced by the commutation relations of the symmetry group associated with the geometric object. Since the symmetry group is determined by the geometry of the shape, the resulting bi-colored graph reflects the intrinsic geometric and algebraic properties of the object. In this sense, the symmetry graph (SG) may be regarded as a combinatorial representation of the commutation structure of the symmetry group.

(ii) Two non-isomorphic geometric shapes may generate isomorphic symmetry Ramsey graphs if their symmetry groups possess identical commutation structures. Therefore, the graph is not necessarily a complete geometric invariant of the shape itself; rather, it is primarily an invariant of the commutation structure of the symmetry group.

(iii) The symmetry operators are usually linear operators acting on a vector space [37]. Suppose a symmetry operation $\hat{S}$ acts on vectors $\vec{x}$ and $\vec{y}$ scalars a, b. Then, linearity means:

$$\hat{S}\left(a\vec{x} + b\vec{y}\right) = a\hat{S}\vec{x} + b\hat{S}\vec{y}. \tag{4}$$

The vector space on which the symmetry operators act is called the representation space of the symmetry group. In geometric applications, this space is typically $\mathbb{R}^2$ or $\mathbb{R}^3$, whereas in quantum mechanics, it is usually a Hilbert space. Some care is necessary when the linearity of symmetry operators is discussed. Not every geometric symmetry is linear in ordinary coordinates. For example, translation T: $(x, y) \to (x + a,\ y + b)$ is affine, not linear, because $T(0, 0) \neq (0, 0)$. The problem is solved if we choose a space describing the object: the symmetry becomes a linear transformation. For example, in homogeneous coordinates, affine transformations, including translations, may be represented by linear matrix operators acting in a higher-dimensional vector space. Thus, geometric symmetries can still be incorporated into the general framework of linear representations of symmetry groups. Therefore, symmetry operations are commonly treated as linear operators within an appropriate representation space, which enables the use of matrix algebra, commutators, eigenvalue analysis, and group representation theory [45].

(iv) The emerging symmetry graph (SG) is generally non-transitive. Consider the example of the regular pentagon. The symmetry group of the regular pentagon is the dihedral group D_5, containing five rotations and five reflections. The rotations commute among themselves, whereas rotations $\hat{r}$ and reflections $\hat{s}$ generally do not commute. Indeed, in D_5, $\hat{s}\hat{r} = \hat{r}^{-1}\hat{s}$, and therefore, $\hat{s}\hat{r} \neq \hat{r}\hat{s}$ for nontrivial rotations $\hat{r}$. Now consider three symmetry operators $\hat{s}, \hat{r}, \hat{r}^2$, where $\hat{s}$ is a reflection and $\hat{r}$ is a nontrivial rotation. The notation $\hat{r}^2$ means the composition (successive application) of the rotation operator with itself. The pairs $(\hat{s}, \hat{r})$ and $(\hat{s}, \hat{r}^2)$ are non-commuting, and therefore, the corresponding edges in the symmetry graph are teal. However, the pair

$(\hat{r}, \hat{r}^2)$ is commuting, and thus, the edge joining them is maroon. Hence, operator $\hat{s}$ is connected by teal edges to both $\hat{r}$ and $\hat{r}^2$, but $\hat{r}$ and $\hat{r}^2$ are connected by a maroon edge. Thus, non-commutation is not transitive in the symmetry graph. This non-transitivity is crucial for further Ramsey-theoretic treatment of the symmetry graphs [46].

(v) The coloring of the symmetry graph is invariant under similarity transformations (invertible changes in representation/basis), including rotations, reflections, translations represented in homogeneous coordinates, and other coordinate transformations acting by conjugation on the symmetry operators.

2.2. Exemplifications of the Ramsey Approach to Symmetry of Shapes

2.2.1. Symmetry Graph of the Equilateral Triangle

The simplest nontrivial example of the introduced approach is supplied by the equilateral triangle. The symmetry group of the equilateral triangle is the dihedral group D_3 containing six symmetry operations:

$$D_3 = \left\{\hat{e}, \hat{r}, \hat{r}^2, \hat{s}_1, \hat{s}_2, \hat{s}_3\right\}, \tag{5}$$

where $\hat{e}$ is the identity operation, $\hat{r}$ is the rotation by $\frac{2\pi}{3}$, $\hat{r}^2$ is the rotation by $\frac{4\pi}{3}$, and $\hat{s}_1, \hat{s}_2, \hat{s}_3$ are reflections about the symmetry axes of the triangle. The group satisfies $\hat{r}^3 = \hat{e}$ and $\hat{s}_i^2 = \hat{e}$. The rotational subgroup $\left\{\hat{e}, \hat{r}, \hat{r}^2\right\}$ is Abelian, since $\hat{r}\hat{r}^2 = \hat{r}^2\hat{r}$. Therefore, the corresponding edges in the symmetry graph are maroon. However, reflections and rotations generally do not commute. Indeed, in D_3, $\hat{s}_i\hat{r} \neq \hat{r}\hat{s}_i$, and the corresponding edges are teal. Moreover, distinct reflections also do not commute: $\hat{s}_i\hat{s}_j \neq \hat{s}_j\hat{s}_i$, $i \neq j$. Thus, the symmetry graph generated by the equilateral triangle is a complete bi-colored graph on six vertices containing both maroon and teal edges.

The symmetry graph of the equilateral triangle is the complete bi-colored graph on six vertices corresponding to the elements of D_3. The identity vertex is connected by maroon edges to all other vertices. The rotational subgroup $\left\{\hat{e}, \hat{r}, \hat{r}^2\right\}$ forms a maroon triangle. Triangles $\{\hat{r}, \hat{s}_1, \hat{s}_2\}$, $\{\hat{r}, \hat{s}_2, \hat{s}_3\}$, $\{\hat{r}, \hat{s}_1, \hat{s}_3\}$, $\{\hat{r}^2, \hat{s}_1, \hat{s}_3\}$, $\{\hat{r}^2, \hat{s}_1, \hat{s}_2\}$, and $\{\hat{r}^2, \hat{s}_2, \hat{s}_3\}$ are teal. Thus, the equilateral triangle already realizes both Ramsey alternatives: a monochromatic commuting triangle and a monochromatic non-commuting triangle. The inevitable appearance of the monochromatic in the SG depicted in Figure 2 illustrates the Ramsey theorem for symmetry graphs.

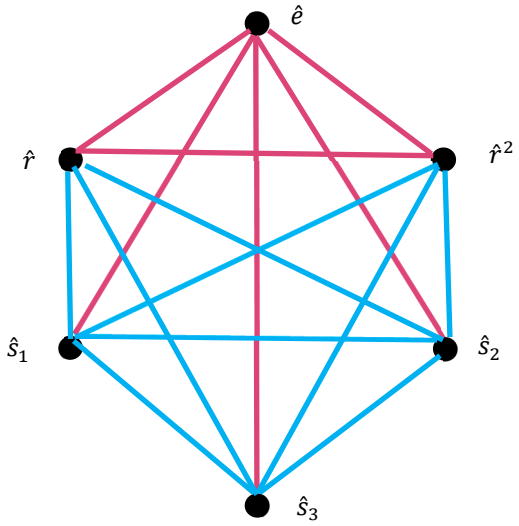

Figure 2. Symmetry graph corresponding to equilateral triangle. Maroon edges correspond to the commuting symmetry operators; teal edges correspond to the non-commuting symmetry operators.

Theorem 1. *Ramsey theorem for symmetry graphs on six vertices.*

Let X be a geometric object whose symmetry group $\mathfrak{H}$ contains at least six symmetry operators. Choose any six distinct operators $\hat{S}_1, \hat{S}_2, \ldots, \hat{S}_6 \in \mathfrak{H}$ and construct the corresponding symmetry graph $SG_6 = (V, E.c)$, where $V = \{\hat{S}_1, \hat{S}_2, \ldots, \hat{S}_6\}$, and every edge is colored maroon if the corresponding operators commute and teal if they do not commute:

$$c = (\hat{S}_i, \hat{S}_j) = \begin{Bmatrix} \text{maroon}, & if\ \hat{S}_i\hat{S}_j = \hat{S}_j\hat{S}_i \\ \text{teal}, & if\ \ \hat{S}_i\hat{S}_j \neq \hat{S}_j\hat{S}_i \end{Bmatrix}.$$

Then, SG_6 necessarily contains at least one monochromatic triangle.

Proof. The symmetry graph SG_6 is a complete graph on six vertices whose edges are colored by two colors: maroon and teal. By the classical Ramsey theorem, $R(3,3) = 6$. Therefore, every two-coloring of the edges of K_6 contains a monochromatic triangle. Here, K_n denotes the complete graph on (n) vertices, i.e., the graph in which every pair of distinct vertices is connected by an edge. Thus, K_6 is the complete graph on six vertices. Since the coloring of SG_6 is a particular two-coloring induced by commutation and non-commutation relations, the result follows immediately. □

The theorem does not depend on the detailed geometry of the object X. It follows only from the fact that the symmetry graph is a complete bi-colored graph on six vertices. However, the actual color pattern is not arbitrary: it is imposed by the algebraic structure of the symmetry group of X. Thus, Ramsey theory guarantees the existence of a monochromatic triangle, while group theory determines which monochromatic triangles actually occur.

Corollary 1. *For every geometric object whose symmetry group contains at least six elements, the commutation structure of its symmetry group necessarily contains one of the following Ramsey substructures:*

- *A triple of pairwise commuting symmetry operators;*
- *A triple of pairwise non-commuting symmetry operators.*

In the case of the equilateral triangle, both alternatives are realized, as can be seen in Figure 2.

It is also noteworthy that we recognize teal quadrangles in the SG depicted in Figure 2, namely, quadrangles $(\hat{r}, \hat{s}_1, \hat{s}_2, \hat{s}_3)$ and $(\hat{r}^2, \hat{s}_1, \hat{s}_2, \hat{s}_3)$. The appearance of teal quadrangles in the symmetry graph reflects higher-order non-commuting substructures within the symmetry group. Whereas teal triangles represent the minimal fully non-commuting subsets of symmetry operators, teal quadrangles reveal larger cyclic incompatibility patterns among symmetry operations. Thus, the teal quadrangles may be interpreted as closed non-commuting symmetry cycles. They represent extended non-Abelian sectors of the symmetry group that cannot be reduced to a single incompatible pair or triangle. In this sense, the quadrangles encode a higher level of algebraic complexity than individual teal edges. It is instructive to build the star-shaped graph emerging for the equilateral triangle, centered around the unity operator $\hat{e}$ [28,29].

Graphs depicted in Figures 2 and 3 demonstrate their own graph-theoretical symmetry, which is called the "second-order symmetry" in the paper. Indeed, the geometric symmetry group $D_3 = \{\hat{e}, \hat{r}, \hat{r}^2, \hat{s}_1, \hat{s}_2, \hat{s}_3\}$ acts on the original object X/equilateral triangle, whereas the automorphism group of the symmetry graph acts on the commutation structure generated by the symmetry operators themselves. Thus, the symmetry graph describes not the primary symmetry of the object, but rather the symmetry of the algebraic relations between symmetry operations. In this sense, the symmetry graph represents a

meta-symmetry structure: a combinatorial symmetry emerging from relations between symmetries themselves.

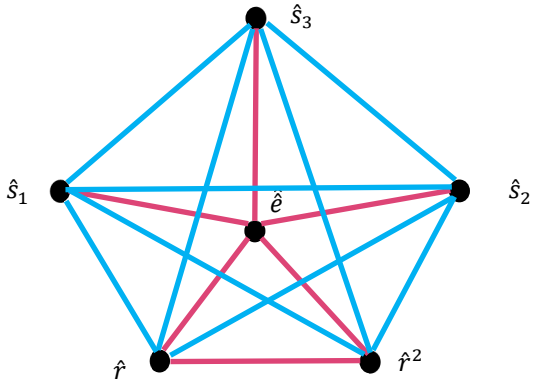

Figure 3. Star-shaped symmetry graph corresponding to equilateral triangle. Maroon edges correspond to the commuting symmetry operators; teal edges correspond to the non-commuting symmetry operators.

Let us discuss the second-order symmetry of the graphs in more detail. Cyclic permutation of the reflections $\hat{s}_1 \to \hat{s}_2 \to \hat{s}_3 \to \hat{s}_1$ preserves the coloring structure. Similarly, interchanging $\hat{r}$ and $\hat{r}^2$ also preserves the graph. Consider that the rotational subgroup $\{\hat{e}, \hat{r}, \hat{r}^2\}$ is Abelian. Therefore, all edges connecting these vertices are maroon. In contrast, reflections generally do not commute with nontrivial rotations, and distinct reflections do not commute with each other. Consequently, most edges involving reflections are teal. Therefore, the symmetry graph inherits automorphisms from the structure of D_3. The identity operator $\hat{e}$ plays a distinguished role. Since $\hat{e}\hat{S} = \hat{S}\hat{e}$, for every symmetry operator $\hat{S}$, the identity vertex is connected by maroon edges to all other vertices. Hence, $\hat{e}$ is the unique universally commuting vertex of the graph. This property becomes especially transparent in the star-shaped graph shown in Figure 3. In that representation, the identity operator serves as the central hub of the graph. Algebraically, this reflects the fact that the identity element belongs to the center of every group. Graph-theoretically, the identity vertex forms a maroon star, $K_{1,5}$, embedded into the complete symmetry graph; $K_{1,5}$ is the star graph consisting of one central vertex connected to five peripheral vertices. It is also noteworthy that the permutation of vertices does not change the number of maroon and teal edges in the graph.

Now, we apply the Mantel–Turán analysis to the symmetry graphs depicted in Figures 2 and 3. Consider a complete bi-colored graph K_n, whose edges are coloured, for example, maroon and teal: let N_m be the number of maroon edges and N_t the number of teal edges. The Mantel–Turán theorem states that if $N_m > \left\lfloor \frac{n^2}{4} \right\rfloor$, then the graph necessarily contains a maroon triangle [27]. Similarly, if $N_t > \left\lfloor \frac{n^2}{4} \right\rfloor$, then the graph necessarily contains a teal triangle. In the graphs depicted in Figures 2 and 3, $N_m = 6$, $N_t = 9$. Now apply Mantel's theorem. A triangle-free graph on six vertices may have at most $\left\lfloor \frac{6^2}{4} \right\rfloor = 9$ edges. Therefore, from the edge count alone, the monochromatic graph with nine edges is exactly at the Mantel threshold. Hence, Mantel's theorem alone does not force a teal or maroon triangle in the graphs. However, the special algebraic structure of D_3 does produce teal and maroon triangles.

Now, remove the identity operator $\hat{e}$ and consider the induced subgraph on the five non-identity vertices: $\{\hat{r}, \hat{r}^2, \hat{s}_1, \hat{s}_2, \hat{s}_3\}$. The only commuting pair within this reduced graph is $(\hat{r}, \hat{r}^2)$. Hence, the reduced teal subgraph contains nine edges out of the ten edges of K_5. Since $\left\lfloor \frac{5^2}{4} \right\rfloor = 6$, Mantel's theorem guarantees, in this case, the existence of at least one teal triangle. Thus, after removal of the identity operator, non-commutativity becomes overwhelmingly dominant within the symmetry graph.

Consider one more instructive example. We address the symmetry of a non-square rectangle. The symmetry group of a non-square rectangle is $D_2 = \left\{\hat{e}, \hat{r}, \hat{h}, \hat{v}\right\}$, where $\hat{e}$ is the identity, $\hat{r}$ is the rotation by π, $\hat{h}$ is the reflection in the horizontal axis, and $\hat{v}$ is the reflection in the vertical axis. This group is Abelian: $\hat{S}_i\hat{S}_j = \hat{S}_j\hat{S}_i$ for all pairs. Therefore, the symmetry Ramsey graph of the rectangle is the complete maroon graph K_4. Thus, the rectangle has a purely Abelian symmetry structure. Its Ramsey graph contains only maroon edges. Geometrically, this means that all elementary symmetry operations of the rectangle are mutually compatible. This leads to the following corollary.

Corollary 2. *If the symmetry group* $\mathfrak{H} = \{\hat{S}_1, \hat{S}_2, \ldots, \hat{S}_n\}$ *is Abelian, then the symmetry Ramsey graph* SG_n *is completely maroon*.

Proof. If $\mathfrak{H} = \{\hat{S}_1, \hat{S}_2, \ldots, \hat{S}_n\}$ is Abelian, then for every pair $\hat{S}_i, \hat{S}_j$, $\hat{S}_i\hat{S}_j = \hat{S}_j\hat{S}_i$. Hence, every edge is maroon. Therefore, SG_n has all maroon edges. □

This applies to rectangles, rhombi with D_2-type symmetry, cyclic rotation groups C_n, and many one-dimensional periodic symmetry groups.

2.2.2. Extension to 3D Shapes and Involving Roto-Inversion

Consider a regular tetrahedron in $\mathbb{R}^3$. If only proper rotations are considered, its symmetry group is $T \simeq A_4$, containing 12 elements. However, if improper symmetries are also included, the full tetrahedral symmetry group is $T_d \simeq S_4$, containing 24 elements. This group contains improper operations, including roto-reflections and roto-inversion-type operations. A roto-inversion operation may be written as $\hat{\bar{R}}_n = \hat{I}\hat{r}_n$, where $\hat{r}_n$ is a rotation about an axis and $\hat{I}$ is spatial inversion: $\hat{I} : \mathrm{x} \mapsto -\mathrm{x}$. Thus, $\hat{\bar{R}}_n : \mathrm{x} \mapsto -R_n\mathrm{x}$. For example, a fourfold roto-inversion is $\hat{\bar{4}} = \hat{I}\hat{R}_{\pi/2}$. Now, choose six symmetry operators from the full tetrahedral symmetry group, for example, $V = \{\hat{e}, \hat{r}, \hat{r}^2, \hat{\sigma}_1, \hat{\sigma}_2, \hat{\bar{R}}\}$, where $\hat{e}$ is the identity, $\hat{r}$ and $\hat{r}^2$ are rotations by $\frac{2\pi}{3}$ and $4\pi/3$, $\hat{\sigma}_1$ and $\hat{\sigma}_2$ are mirror reflections, and $\hat{\bar{R}}$ is a roto-inversion operator. A symmetry graph constructed on these six vertices, with coloring edges by commutation relations, is supplied in Appendix A. The corresponding graph is depicted in Figure 4.

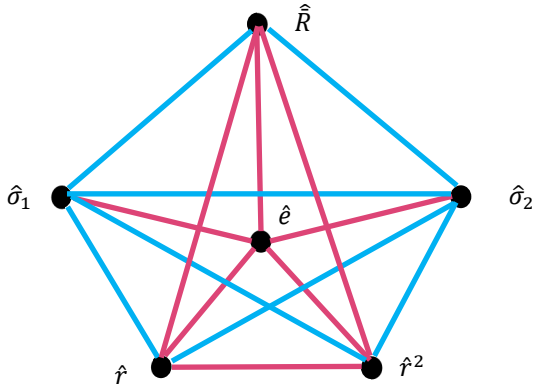

Figure 4. Symmetry graph emerging from six symmetry operators taken from the full tetrahedral symmetry group $V = \left\{\hat{e}, \hat{r}, \hat{r}^2, \hat{\sigma}_1, \hat{\sigma}_2, \hat{\bar{R}}\right\}$. Maroon edges correspond to the commuting symmetry operators; teal edges correspond to the non-commuting symmetry operators.

So, SG, depicted in Figure 4, contains the maroon triangles $(\hat{e}, \hat{r}, \hat{r}^2)$, $(\hat{r}, \hat{r}^2, \hat{\bar{R}})$, $(\hat{e}, \hat{r}, \hat{\bar{R}})$, and $(\hat{e}, \hat{r}^2, \hat{\bar{R}})$ and the teal triangles $(\hat{\sigma}_1, \hat{\sigma}_2, \hat{\bar{R}})$, $(\hat{r}, \hat{\sigma}_1, \hat{\sigma}_2)$, and $(\hat{r}^2, \hat{\sigma}_1, \hat{\sigma}_2)$. The simultaneous appearance of maroon and teal monochromatic triangles reveals an important structural property of the symmetry group. Maroon triangles correspond to triples of mutually com-

muting symmetry operators. Such subsets form locally compatible symmetry substructures, in which the order of application of the symmetry operations is irrelevant. In contrast, teal triangles correspond to triples of pairwise non-commuting symmetry operators. These subsets represent intrinsically non-Abelian symmetry structures for which the order of operations is essential.

Thus, the symmetry graph decomposes the symmetry group into commuting and non-commuting Ramsey substructures. The coexistence of maroon and teal triangles demonstrates that the tetrahedral symmetry group simultaneously contains locally Abelian and intrinsically non-Abelian sectors. From the Ramsey-theoretic viewpoint, monochromatic triangles emerge as inevitable elementary commutation patterns within sufficiently rich symmetry groups. The appearance of teal triangles involving reflections and roto-inversion operations indicates that improper symmetries are a natural source of non-commutativity in three-dimensional geometry. Therefore, the symmetry graph provides a compact combinatorial representation of the algebraic complexity of spatial symmetry groups.

2.2.3. Applications of Symmetry Graph to Crystallography

Let us apply the developed approach to crystallography. Consider trigonal crystal structures, the symmetry of which is characterized by the dihedral group $D_3 \cong C_{3v}$. The six symmetry operations are $C_{3v} = \{\hat{e}, \hat{r}, \hat{r}^2, \hat{\sigma}_1, \hat{\sigma}_2, \hat{\sigma}_3\}$, where $\hat{e}$ is the identity; $\hat{r}$ is the rotation by $\frac{2\pi}{3}$; $\hat{r}^2$ is the rotation by $\frac{4\pi}{3}$; and $\hat{\sigma}_1, \hat{\sigma}_2, \hat{\sigma}_3$ are mirror reflections. This is algebraically identical to the symmetry group of the equilateral triangle discussed in Section 2.2.1. Thus, the corresponding crystallographic symmetry graph contains: six vertices; maroon edges joining commuting operations; and teal edges joining non-commuting operations. The rotational subgroup $\{\hat{e}, \hat{r}, \hat{r}^2\}$ forms a maroon triangle because it is Abelian. The reflections do not commute with the nontrivial rotations $\hat{\sigma}_i\hat{r} \neq \hat{r}\hat{\sigma}_i, i = 1, \ldots, 3$ and therefore generate teal edges.

Distinct reflections also do not commute: $\hat{\sigma}_i\hat{\sigma}_j \neq \hat{\sigma}_j\hat{\sigma}_i, i \neq j$. Consequently, the crystallographic symmetry graph generated by C_{3v} is exactly the same type of complete bi-colored graph analyzed in the equilateral triangle example. Thus, the crystallographic point group C_{3v} naturally generates a complete bi-colored symmetry graph on six vertices containing both commuting and non-commuting monochromatic triangles. This example demonstrates that the Ramsey approach to symmetry applies naturally to crystallographic point groups.

2.2.4. Extension of the Symmetry Graphs to Infinite Tilings

Now, we extend the suggested approach to infinite tilings. As an example, we develop SG for the Cairo tiling [47,48]. The Cairo pentagonal tiling, denoted T_C, is an edge-to-edge tessellation of the Euclidean plane $\mathbb{R}^2$ by congruent convex pentagons, called Cairo pentagons, such that:

(i) Every tile is a convex pentagon possessing two equal adjacent sides and three additional equal sides;
(ii) The pentagons cover the plane completely, $\bigcup_{P_i \in T_C} P_i = \mathbb{R}^2$;
(iii) The interiors of distinct pentagons are disjointed, $\mathrm{Int}(P_i) \cap \mathrm{Int}(P_j) = \emptyset$, $i \neq j$;
(iv) Adjacent pentagons meet only along complete edges or vertices;
(v) The standard Cairo pentagon has angles $\frac{2\pi}{3}$; $\frac{2\pi}{3}$, $\frac{\pi}{2}$; $\frac{2\pi}{3}$; and $\frac{\pi}{2}$. Consequently, three $\frac{2\pi}{3}$ angles may meet at one type of vertex, whereas four $\frac{\pi}{2}$ angles may meet at another type of vertex (see Figure 5). This mixed local structure is one of the features distinguishing the Cairo pentagonal tiling from regular tilings by equilateral triangles, squares, or regular hexagons.

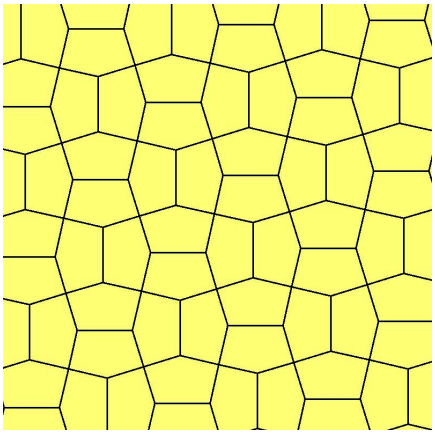

Figure 5. Cairo tiling is depicted. Cairo tiling is made of congruent convex pentagons.

The tiling is periodic and possesses translational symmetry in two independent directions. The full symmetry group of the ideal Cairo tiling is a wallpaper group generated by translations together with rotations, reflections, and glide reflections preserving the tessellation. The Cairo tiling derives its name from the characteristic paving patterns widely used in the streets and sidewalks of Cairo.

Consider the symmetries of the Cairo tiling. Let T_C denote the Cairo pentagonal tiling. Its symmetry group is $G(T_C) = \{S : \mathbb{R}^2 \to \mathbb{R}^2 \mid S(T_C) = T_C\}$. For the standard periodic Cairo tiling, the symmetry operators are the following Euclidean isometries: (i) Identity operator $\hat{e} : \mathrm{x} \mapsto \mathrm{x}$. This operator leaves every point fixed. (ii) Translation operators: Since the Cairo tiling is periodic, it has two independent translation vectors $\vec{a}$ and $\vec{b}$. Thus, for all integers $m, n \in \mathbb{Z}$, $\hat{T}_{m,n} : \mathrm{x} \mapsto \mathrm{x} + m\vec{a} + n\vec{b}$. These translations generate an infinite countable subgroup. (iii) Rotation operators: The standard Cairo tiling has fourfold rotational symmetry. Therefore, it contains rotations by $\frac{\pi}{2}$, π, $\frac{3\pi}{2}$ about appropriate rotation centers. Thus, we introduce the operator $\hat{R}_{P,k} : \mathrm{x} \mapsto P + Q_k(\mathrm{x} - P)$, where P is a rotation center, $k = 1, 2, 3$, and Q_k is the rotation matrix through angle $k\pi/2$. There are also half-turns, i.e., rotations by π, about suitable centers of the tiling. The wallpaper group $p4g$ contains fourfold and twofold rotation centers. (iv) Reflection operators: The Cairo tiling also contains mirror symmetries. A reflection operator has the form $\hat{M}_\ell : \mathrm{x} \mapsto$ reflection of x in the line ℓ, where ℓ is a mirror axis of the tiling. For the $p4g$ symmetry type, the reflection axes occur in two perpendicular directions. (v) Glide-reflection operators: In addition to ordinary reflections, the Cairo tiling contains glide reflections. A glide reflection is a composition of a reflection in a line ℓ and a translation parallel to that line, $\hat{G}_{\ell,\mathrm{u}} = \hat{T}_{\vec{u}} \circ \hat{M}_\ell$, where $\vec{u}$ is parallel to ℓ. For the $p4g$ wallpaper group, glide-reflection axes occur parallel to reflection axes and also in diagonal directions. Thus, the full symmetry group may be written schematically as:

$$\mathfrak{H}(T_C) = \left\{\hat{e},\ \hat{T}_{m,n},\ \hat{R}_{P,k},\ \hat{M}_\ell,\ \hat{G}_{\ell,\vec{u}}\right\},\ \ m, n \in \mathbb{Z},\ k = 1, 2, 3. \tag{6}$$

Since the Cairo pentagonal tiling is periodic, its full symmetry group $\mathfrak{H}(T_C)$ is an infinite wallpaper group. The commutation rules for the aforementioned symmetry operations are summarized in Appendix B. This group is countable, because its translational part is generated by two independent lattice translations, and the remaining point-symmetry operations form a finite set. Therefore, the associated symmetry graph $SG_\infty(T_C)$ is a countably infinite complete bi-colored graph. The infinite Ramsey theorem is applicable: every countably infinite complete graph whose edges are colored by a finite amount of colors contains an infinite monochromatic complete subgraph. In the present case, this theorem implies that

the symmetry graph of the Cairo tiling contains an infinite monochromatic clique. Moreover, this clique is realized explicitly by the translation subgroup $\mathcal{T} = \left\{ T_x^m T_y^n : m, n \in \mathbb{Z} \right\}$, which is Abelian. Hence every pair of translations commutes, and the corresponding vertices form an infinite maroon clique.

The infinite Ramsey theorem for symmetry graphs is formulated as follows:

Theorem 2. *Infinite Ramsey theorem for symmetry graphs.*

Let X be a geometric object or tiling whose symmetry group $\mathfrak{H}$ contains a countably infinite amount of symmetry operators, $\mathfrak{H} = \{\hat{S}_1, \hat{S}_2, \hat{S}_3, \ldots\}$. Construct the infinite symmetry graph $SG_\infty = (V, E, c)$, where $V = \mathfrak{H}$, and every pair of distinct symmetry operators is connected by an edge (see Figure 6). The coloring function is defined by:

$$c(\hat{S}_i, \hat{S}_j) = \begin{cases} \text{maroon}, & \hat{S}_i\hat{S}_j = \hat{S}_j\hat{S}_i, \\ \text{teal}, & \hat{S}_i\hat{S}_j \neq \hat{S}_j\hat{S}_i. \end{cases}$$

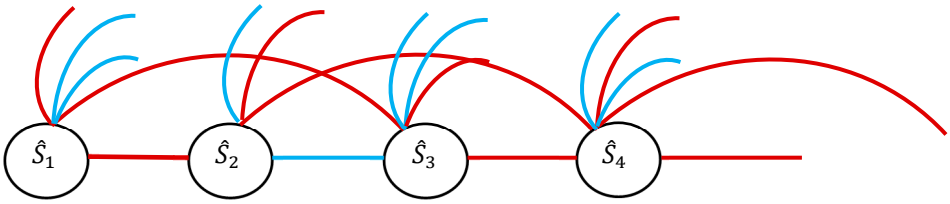

Figure 6. Infinite Ramsey theorem is illustrated for twin-colored infinite symmetry graphs SG_∞. Maroon edges correspond to the commuting symmetry operators; teal edges correspond to the non-commuting symmetry operators. Any two-colored infinite symmetry graph must contain a maroon or teal monochromatic countably infinite complete subgraph. Infinite subset of vertices whose pairwise edges all have the same color is necessarily present.

Then, SG_∞ contains an infinite monochromatic complete subgraph. Equivalently, there exists an infinite subset $\mathfrak{H}' \subset \mathfrak{H}$, $|\ \mathfrak{H}'\ | = \infty$, such that one of the following alternatives holds: $\hat{S}_i\hat{S}_j = \hat{S}_j\hat{S}_i$ for all $\hat{S}_i, \hat{S}_j \in \mathfrak{H}'$, or $\hat{S}_i\hat{S}_j \neq \hat{S}_j\hat{S}_i$ for all distinct $\hat{S}_i, \hat{S}_j \in \mathfrak{H}'$.

Thus, every infinite symmetry graph contains either an infinite family of pairwise commuting symmetry operators or an infinite family of pairwise non-commuting symmetry operators.

Proof. The graph SG_∞ is a complete graph on a countably infinite set of vertices, and its edges are colored by two colors according to the commutation relation of the corresponding symmetry operators. Therefore, the classical infinite Ramsey theorem applies. It guarantees the existence of an infinite subset of vertices whose pairwise edges all have the same color. Translating this result back into the language of symmetry operators gives either an infinite pairwise commuting family or an infinite pairwise non-commuting family. □

For periodic tilings, such as the Cairo pentagonal tiling, the symmetry group is infinite, because it contains an infinite amount of translations. Therefore, its symmetry graph is naturally infinite. The infinite Ramsey theorem then implies that the commutation structure of the tiling necessarily contains an infinite monochromatic symmetry substructure.

2.2.5. Semi-Transitive Symmetry Graphs

One-dimensional symmetry represents a particular but important case, leading to somewhat surprising results. Consider a one-dimensional (1D) set of points. The operators of symmetry are: (i) translations: $\hat{T}_a(x) = x + a$; (ii) reflections: $\hat{S}_p(x) = 2p - x$. Take the five vertices $V = \{\hat{T}_a, \hat{T}_b, \hat{T}_c, \hat{S}_p, \hat{S}_q\}$ and assume $a, b, c \neq 0$, $p \neq q$. It should be

emphasized that the selected finite set of operators is not closed under composition and therefore does not constitute a group.

The full commutation list is: $[\hat{T}_a, \hat{T}_b] = 0$, $[\hat{T}_a, \hat{T}_c] = 0$, $[\hat{T}_b, \hat{T}_c] = 0$, $[\hat{T}_a, \hat{S}_p] \neq 0$, $[\hat{T}_b, \hat{S}_p] \neq 0$, $[\hat{T}_c, \hat{S}_p] \neq 0$, $[\hat{T}_a, \hat{S}_q] \neq 0$, $[\hat{T}_b, \hat{S}_q] \neq 0$, $[\hat{T}_c, \hat{S}_q] \neq 0$, $[\hat{S}_p, \hat{S}_q] \neq 0$ (see Appendix C). The corresponding SG is presented in Figure 7. It is easily seen that commuting operators are transitive within this graph, whereas non-commuting operators are non-transitive. Thus, a semi-transitive, bi-colored complete graph emerges [46,49].

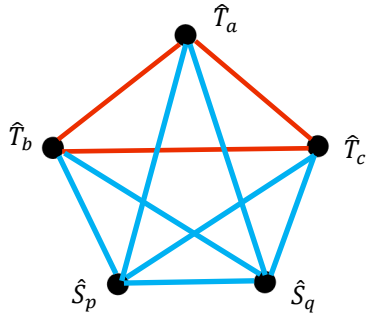

Figure 7. Symmetry graph emerging for 1D translations and reflections. Maroon edges connect the commuting symmetry operators; teal edges correspond to the non-commuting symmetry operators.

It was demonstrated that the Ramsey number for semi-transitive graphs $R_{semi-trans}(3,3) = 5$. Indeed, we recognize from Figure 7 that the triangle $\{\hat{T}_a, \hat{T}_b, \hat{T}_c\}$ is maroon and the triangles $\{\hat{T}_a, \hat{S}_p, \hat{S}_q\}$, $\{\hat{T}_b, \hat{S}_p, \hat{S}_q\}$, and $\{\hat{T}_c, \hat{S}_p, \hat{S}_q\}$ are teal. This stands in sharp contrast with the aforementioned non-transitive SG, for which $R(3,3) = 6$. It is noteworthy that 1D problems often give rise to semi-transitive graphs [49]. The dimensionality of the system appears to constrain the logical structure of the associated Ramsey graph. In one-dimensional systems, compatibility relations are often governed by a single scalar parameter or by simple Abelian structures, naturally generating semi-transitive graphs. This observation calls for future investigations.

3. Extension to Physics: Ising Ferromagnet

Now, we extend the developed approach to physics. Consider the ferromagnetic Ising model on a lattice with the Hamiltonian:

$$H = -J \sum_{\langle i,j \rangle} \sigma_i \sigma_j, \tag{7}$$

where J is the exchange interaction constant (coupling parameter) between neighboring spins, and $\sigma_i = \pm 1$ denotes the Ising spin variable at lattice site i. The system possesses an intrinsic discrete symmetry: $\sigma_i \to -\sigma_i$. Now consider a finite Ising system possessing additional discrete spatial symmetries, for example: lattice reflections, lattice inversions, discrete translations under periodic boundary conditions, and discrete rotations of the lattice. These operators are genuine physical symmetries of the Hamiltonian. As an example, we address specific lattice cells of the triangular Ising trimer. Consider three identical Ising spins placed at the vertices of an equilateral triangle: $\sigma_1, \sigma_2, \sigma_3 = \pm 1$. Let the Hamiltonian be:

$$H = -J(\sigma_1\sigma_2 + \sigma_2\sigma_3 + \sigma_3\sigma_1). \tag{8}$$

This system has the discrete symmetry group:

$$D_3 = \left\{\hat{e}, \hat{r}, \hat{r}^2, \hat{s}_1, \hat{s}_2, \hat{s}_3\right\}, \tag{9}$$

where $\hat{r}$ is the rotation by $2\pi/3$, and $\hat{s}_1, \hat{s}_2, \hat{s}_3$ are reflections permuting the spin sites. These are genuine physical symmetry operators because they leave the Hamiltonian invariant: $H(\hat{S}\sigma) = H(\sigma), S \in D_3$. Thus, the symmetry graph has exactly six vertices:

$$V = \left\{\hat{e}, \hat{r}, \hat{r}^2, \hat{s}_1, \hat{s}_2, \hat{s}_3\right\}. \tag{10}$$

The rotational subgroup $\left\{\hat{e}, \hat{r}, \hat{r}^2\right\}$ is Abelian, so it gives maroon edges. However,

$$\hat{s}_i\hat{r} \neq \hat{r}\hat{s}_i, \tag{11}$$

and distinct reflections also generally do not commute:

$$\hat{s}_i\hat{s}_j \neq \hat{s}_j\hat{s}_i, i \neq j. \tag{12}$$

Therefore, the graph also contains teal edges. The resulting SG coincides with that depicted in Figure 3. The reason is that both systems possess the same symmetry group D_3 and, consequently, the same commutation structure between symmetry operators. Indeed, the equilateral triangle and the triangular Ising trimer are governed by identical algebraic relations between rotations and reflections: $\hat{r}^3 = \hat{e}$, $\hat{s}_i^2 = \hat{e}$, $\hat{s}_i\hat{r} = \hat{r}^{-1}\hat{s}_i$. Therefore, the coloring rules of the corresponding symmetry graphs are identical. The rotational subgroup $\left\{\hat{e}, \hat{r}, \hat{r}^2\right\}$ is Abelian in both systems and generates the same maroon triangle, whereas reflections do not commute with nontrivial rotations and therefore generate identical teal substructures. Hence, the resulting symmetry graph is a complete bi-colored graph on six vertices. By the Ramsey theorem $R(3,3) = 6$, this physical symmetry graph necessarily contains at least one monochromatic triangle. Thus, the triangular Ising trimer supplies a concrete non-continuous, non-crystallographic physical realization of the six-vertex Ramsey symmetry graph. Hence, the symmetry graph depends primarily on the commutation structure of the symmetry group rather than on the physical nature of the underlying system itself. This observation demonstrates that symmetry graphs are algebraic-combinatorial invariants of symmetry groups. Physically very different systems may generate isomorphic symmetry graphs whenever their symmetry groups possess identical commutation structures. Thus, the introduced Ramsey framework reveals universal combinatorial structures shared by geometry, crystallography, and statistical physics.

4. Symmetry Graph Emerging from the Motion in the Central Field

Consider a nonrelativistic quantum particle of mass m moving in a central potential $\varphi(r)$:

$$\hat{H} = \frac{\hat{\mathrm{p}}^2}{2m} + \varphi(r). \tag{13}$$

Since $\varphi(r)$ depends only on the distance from the origin, the Hamiltonian is invariant under all spatial rotations. Thus, every rotation operator $\hat{R} \in SO(3)$ is a symmetry operation of the Hamiltonian. The continuous group $SO(3)$ is non-Abelian, namely:

$$\hat{r}_x(\alpha)\hat{r}_y(\beta) \neq \hat{r}_y(\beta)\hat{r}_x(\alpha), \tag{14}$$

where $\hat{r}_x(\alpha)$ denotes the rotation about axis x by angle α. We now discretize the problem and construct a finite induced symmetry graph by choosing:

$$V = \left\{\hat{r}_x(\pi), \hat{r}_y(\pi), \hat{r}_z(\pi), \hat{r}_x(\pi/2), \hat{r}_y(\pi/2), \hat{r}_z(\pi/2)\right\}. \tag{15}$$

Two vertices of this graph are connected by a maroon edge when the corresponding rotations commute and by a teal edge when they do not commute. The half-turns $\hat{r}_x(\pi), \hat{r}_y(\pi)$, and $\hat{r}_z(\pi)$ commute pairwise and therefore form a maroon triangle. Each half-turn also commutes with the quarter-turn about the same axis. In contrast, rotations about different axes generally do not commute; hence, the corresponding edges are teal. Thus, the symmetry graph reflects the non-Abelian structure of the rotational symmetry group $SO(3)$, while all vertices remain genuine symmetry operations of the central-field Hamiltonian. The graph contains the maroon triangle $\{\hat{r}_x(\pi),\ \hat{r}_y(\pi),\ \hat{r}_z(\pi)\}$ and teal triangles $\{\hat{r}_x(\pi),\ \hat{r}_y(\pi/2),\ \hat{r}_z(\pi/2)\}$, $\{\hat{r}_y(\pi),\ \hat{r}_x(\pi/2),\ \hat{r}_z(\pi/2)\}$, $\{\hat{r}_z(\pi),\ \hat{r}_x(\frac{\pi}{2}),\ \hat{r}_y(\frac{\pi}{2})\}$, and $\{\hat{r}_x(\pi/2),\ \hat{r}_y(\pi/2),\ \hat{r}_z(\pi/2)\}$.

Physically, this means that finite rotations in three-dimensional space depend on the order in which they are performed; equivalently, spatial orientation changes are path-dependent. The symmetry graph converts this group-theoretic property into a concrete combinatorial structure. The induced symmetry graph contains 15 edges. Among them, six are maroon and nine are teal. Since the Mantel–Turán bound for triangle-free graphs on six vertices is $\left\lfloor \frac{6^2}{4} \right\rfloor = 9$, the teal subgraph has exactly the extremal number of edges. However, it is not triangle-free. Thus, the existence of monochromatic triangles in this particular graph is not forced by the Mantel–Turán edge count criterion alone but follows from the specific commutation structure of the selected rotations. Direct inspection gives one maroon triangle and four teal triangles. Thus, the symmetry graph transforms the algebraic structure of rotational invariance into a combinatorial object, enabling the identification of commuting and non-commuting symmetry substructures within the same rotationally invariant physical system.

5. Jacobi Identity for Symmetry Operators

Since symmetry operators may be represented as linear operators on a representation space, their commutator is defined as $[\hat{S}_i, \hat{S}_j] = \hat{S}_i\hat{S}_j - \hat{S}_j\hat{S}_i$. For any three linear operators $\hat{S}_i, \hat{S}_j,$ and $\hat{S}_k$, the commutator satisfies the Jacobi identity:

$$[\hat{S}_i, [\hat{S}_j, \hat{S}_k]] + [\hat{S}_j, [\hat{S}_k, \hat{S}_i]] + [\hat{S}_k, [\hat{S}_i, \hat{S}_j]] = 0. \tag{16}$$

The symmetry graphs introduced in Sections 2 and 3 are constructed from symmetry operators regarded as elements of a symmetry group, with edge coloring determined by commutation or non-commutation relations. However, the Jacobi identity is not an identity of abstract groups themselves. It arises naturally only after passing to a linear operator framework, such as a matrix representation algebra or the group algebra generated by the symmetry operators. Therefore, in the present section, the symmetry operators are embedded into an associative algebra acting on a representation space. The commutator is then defined in the usual operator-theoretic sense.

Consider a set of symmetry operators $\mathfrak{H} = \{\hat{S}_1, \hat{S}_2, \ldots, \hat{S}_N\}$. Two very different situations are possible: (1) The set $\mathfrak{H}$ is supposed to be commutation-closed, namely, for all i and j $[\hat{S}_i, \hat{S}_j] = 0$ or $[\hat{S}_i, \hat{S}_j] \in span\{\hat{S}_1, \hat{S}_2, \ldots, \hat{S}_N\}$ for any $i, j = 1, \ldots, N$ (the set is Lie-closed up to linear span), or (2) the set $\mathfrak{H}$ is not commutation-closed, i.e., exists with at least one pair of i and j for which $[\hat{S}_i, \hat{S}_j] = \hat{W}$ and $\hat{W} \notin span\{\hat{S}_1, \hat{S}_2, \ldots, \hat{S}_N\}$. We also suppose that there exists at least one pair of operators $\hat{S}_{i_1}$ and $\hat{S}_{i_2}$ such that $[\hat{S}_{i_1}, \hat{S}_{i_2}] \neq 0$, indicating that not all operators in the set commute. This implies that this subalgebra of operators is nontrivial, with non-zero commutation relations between some operators. To formulate Jacobi-type constraints, the symmetry operators are embedded into the associative algebra (or matrix representation algebra) generated by the symmetry group. The corresponding commutation pattern may be represented combinatorially by the associated SG. The Jacobi

identity then constrains the operator-algebraic relations associated with this commutation pattern, such as when the set contains three operators, and say, the commutation relations satisfy $[\hat{S}_1, \hat{S}_2] = [\hat{S}_1, \hat{S}_3] = 0$; $[\hat{S}_2, \hat{S}_3] \neq 0$. These commutation relations give rise to the SG depicted in Figure 8. If the set $\mathfrak{H} = \{\hat{S}_1, \hat{S}_2, \hat{S}_3\}$ is commutation-closed (Lie-closed), the Jacobi identity is trivial (this is easily checked by direct substitution of the operators into the Jacobi identity). In contrast, if the set $\mathfrak{H} = \{\hat{S}_1, \hat{S}_2, \hat{S}_3\}$ is not commutation-closed, the Jacobi identity yields $[\hat{S}_1, [\hat{S}_2, \hat{S}_3]] = 0$, which is nontrivial.

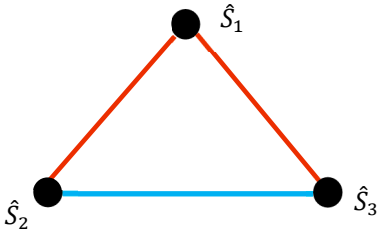

Figure 8. Symmetry graph emerging for the set of three symmetry operators. The commutation relations are: $[\hat{S}_1, \hat{S}_2] = [\hat{S}_1, \hat{S}_3] = 0$; $[\hat{S}_2, \hat{S}_3] \neq 0$.

Equation $[\hat{S}_1, [\hat{S}_2, \hat{S}_3]] = 0$ says that the operator $[\hat{S}_2, \hat{S}_3]$ lies in the centralizer of $\hat{S}_1$. Let us explain how the Jacobi identity works. The example is supplied by the group D_3, represented by permutation matrices (see Section 2.2). We assume: $\hat{S}_1 = \hat{r} + \hat{r}^2$, $\hat{S}_2 = \hat{s}_1$, and $\hat{S}_3 = \hat{s}_2$ ($\hat{s}_i$, $i = 1, 2$ are reflections). Consider that $\hat{S}_1 = \hat{r} + \hat{r}^2$ are algebra elements rather than group elements. Because distinct reflections in D_3 do not commute, $[\hat{s}_1, \hat{s}_2] \neq 0$. However, the symmetric rotational combination $\hat{r} + \hat{r}^2$ commutes with both reflections. Using the relation $\hat{s}\hat{r} = \hat{r}^{-1}\hat{s}$, we obtain:

$$\hat{s}_i\left(\hat{r} + \hat{r}^2\right) = \left(\hat{r}^2 + \hat{r}\right)\hat{s}_i = \left(\hat{r} + \hat{r}^2\right)\hat{s}_i, \tag{17}$$

and therefore:

$$\left[\hat{r} + \hat{r}^2, \hat{s}_1\right] = 0, \left[\hat{r} + \hat{r}^2, \hat{s}_2\right] = 0. \tag{18}$$

Consequently, the Jacobi identity yields:

$$\left[\hat{r} + \hat{r}^2, [\hat{s}_1, \hat{s}_2]\right] = 0. \tag{19}$$

For discrete symmetry groups, the Jacobi identity generally becomes structurally nontrivial only after passing from the group itself to the associative or Lie algebra generated by its matrix representation (see Appendix D). Therefore, higher-order constraints on symmetry graphs arise naturally in the Lie-closed extension of the symmetry graph. In this extended framework, the Jacobi identity constrains the propagation of non-commutativity and reveals hidden algebraic organization underlying the teal subgraph. Thus, the Lie-closed symmetry graph combines the Ramsey-type combinatorial structure with higher-order Lie-algebraic consistency conditions.

6. Discussion

The present work introduces a Ramsey-theoretic formulation of symmetry theory. Symmetry operations were treated as operators forming vertices of complete bi-colored graphs, whereas commutation and non-commutation relations induced the corresponding edge coloring. This construction transforms the algebraic structure of symmetry groups into combinatorial objects suitable for graph-theoretical and Ramsey-theoretical analysis.

The obtained symmetry graphs are not arbitrary edge-colored graphs. Their coloring is constrained by the algebraic structure of the underlying symmetry groups. In this

sense, symmetry graphs may be regarded as combinatorial representations of commutation structures arising in geometry, crystallography, tiling theory, and physics. The introduced framework establishes a bridge between group theory, operator algebra, graph theory, and Ramsey combinatorics.

A central result of the present work is the appearance of unavoidable monochromatic structures in symmetry graphs. For symmetry groups containing at least six elements, the classical Ramsey theorem guarantees the existence of monochromatic commuting or non-commuting triangles. The equilateral triangle, tetrahedral symmetry group, crystallographic point groups, and Ising trimer all demonstrate explicit realizations of these Ramsey substructures.

The physical and algebraic interpretation of the monochromatic subgraphs is important. Maroon monochromatic triangles correspond to locally Abelian sectors of the symmetry group, where the order of application of symmetry operations is irrelevant. In contrast, teal monochromatic triangles correspond to intrinsically non-Abelian sectors characterized by pairwise non-commuting symmetry operators. Thus, the symmetry graph naturally decomposes the symmetry group into compatible and incompatible operator substructures. This decomposition may be useful for the analysis of large symmetry structures, because it transforms local commutation relations into a global combinatorial object.

Although the commutation structure is already encoded in the symmetry group, the graph representation reorganizes this information into a global combinatorial object amenable to graph-theoretic analysis. In particular, complete maroon subgraphs correspond to mutually commuting families of symmetry operators, whereas complete teal subgraphs identify intrinsically non-Abelian sectors. This representation facilitates the identification of maximal commuting subsets, strongly non-commuting sectors, and higher-order compatibility patterns that may be difficult to recognize directly from multiplication tables or individual commutation relations. Moreover, the graph formulation enables the application of Ramsey-theoretic, clique-detection, and extremal graph-theoretic methods to symmetry-generated operator systems.

A simple illustration of the usefulness of this viewpoint is provided by Theorem 1. Consider six symmetry operators selected from a symmetry group. In the original algebraic formulation, their commutation properties appear as a collection of pairwise relations. In contrast, once the operators are represented as vertices of a symmetry graph, the classical Ramsey theorem immediately guarantees the existence of either a triple of pairwise commuting operators or a triple of pairwise non-commuting operators. This conclusion emerges from a general combinatorial principle rather than from direct inspection of the multiplication table of the group. More generally, Ramsey-theoretic and extremal graph-theoretic techniques provide a natural framework for identifying and classifying compatible and incompatible operator sectors. Thus, the symmetry graph does not introduce additional algebraic information, but it enables the extraction of global structural properties from commutation data through combinatorial methods.

The appearance of higher-order monochromatic structures, such as teal quadrangles, reveals more extended non-commuting compatibility cycles within symmetry groups. These structures encode algebraic complexity beyond individual commutation relations and reflect the non-Abelian generator structure of the group itself. The mathematical novelty of the work therefore does not lie in the introduction of commutation relations themselves, which are classical [19–25], but rather in their reformulation within a Ramsey-theoretic framework, i.e., the paper re-shapes symmetry considerations in the terms of the Ramsey theory [26,41]. In particular, the paper applies Ramsey theory to symmetry-generated operator structures, interprets monochromatic subgraphs as algebraically meaningful commuting or non-commuting sectors, extends the construction to infinite symmetry groups

and tilings via the infinite Ramsey theorem, and discusses higher-order combinatorial structures such as teal quadrangles and second-order graph symmetries. Thus, the work should be viewed as a Ramsey-theoretic and combinatorial extension of classical commuting-graph ideas to symmetry groups and physical symmetry operators.

An important aspect of the proposed framework is the emergence of "second-order symmetry." The original symmetry group acts on the geometric or physical object itself, whereas the automorphism group of the symmetry graph acts on the commutation structure generated by the symmetry operators. Thus, the symmetry graph represents a meta-symmetry structure: a combinatorial symmetry of relations between symmetries. The notion termed here "second-order symmetry" is closely related to the standard graph-theoretic concept of the automorphism group of a graph. In the present framework, the symmetry graph is a complete bi-colored graph; therefore, its automorphisms are color-preserving permutations of vertices preserving commutation and non-commutation relations between symmetry operators. Thus, $\mathrm{Aut}(SG)$ describes symmetries of the commutation structure itself. This treatment connects naturally to the established theory of graph automorphisms and symmetries of colored graphs [26–30].

An additional advantage of the graph-theoretical formulation is that it remains meaningful even when the selected set of symmetry operators is not closed under composition and therefore does not itself form a group. Classical group-theoretic methods rely essentially on closure and the full multiplication structure of the group. In contrast, the symmetry graph requires only pairwise commutation information and may therefore be constructed for arbitrary collections of symmetry operators. This makes it possible to apply Ramsey-theoretic and extremal graph-theoretic methods to operator sets that lie outside the standard framework of group theory. In particular, monochromatic cliques, non-commuting sectors, and other higher-order combinatorial structures may be identified even when no underlying group structure is present. Thus, the symmetry graph should be viewed not only as a representation of symmetry groups but also as a more general tool for analyzing commutation patterns within collections of symmetry operators.

The introduced approach naturally extends beyond finite groups. Infinite periodic tilings, such as the Cairo pentagonal tiling, generate countably infinite symmetry graphs. In this case, the infinite Ramsey theorem guarantees the existence of infinite monochromatic commuting or non-commuting substructures. The translational subgroup of the Cairo tiling explicitly realizes an infinite maroon clique corresponding to an infinite family of mutually commuting translations.

The developed framework also extends naturally to physical systems. The triangular Ising trimer provides a physical realization of the same symmetry graph generated by the equilateral triangle, because both systems possess identical commutation structures of symmetry operators. This demonstrates that symmetry graphs depend primarily on the algebraic commutation structure of the symmetry group rather than on the detailed physical nature of the underlying system. Consequently, physically different systems may generate isomorphic symmetry graphs.

The Lie-algebraic extension considered through the Jacobi identity demonstrates that symmetry graphs possess additional higher-order algebraic constraints whenever the operator set is commutation-closed. In this sense, the developed framework combines Ramsey-type combinatorial inevitability with Lie-algebraic consistency conditions. The Jacobi identity constrains the propagation of non-commutativity and reveals hidden algebraic organization inside the teal subgraph.

The present work may be extended in multiple directions. Possible developments include applications to crystallographic space groups, Lie groups, quantum symmetry operators, gauge symmetries, topological phases, operator algebras, and dynamical symmetry

groups in classical and quantum mechanics. Multi-colored symmetry graphs based on refined compatibility relations may also be considered.

The extension of the symmetry-graph framework to infinite and continuous symmetry groups also has several limitations. For finite groups, the symmetry graph is a finite complete bi-colored graph, and classical finite Ramsey results apply directly. In contrast, continuous Lie groups such as $SO(3)$, $SU(2)$, or gauge symmetry groups contain an uncountable amount of symmetry operators. The corresponding symmetry graph is therefore uncountably infinite, making explicit graph construction and visualization impossible in practice. Consequently, continuous groups are typically analyzed through finite induced subgraphs generated by selected representative symmetry operations. This procedure was employed in Section 4, where the continuous Lie group $SO(3)$ was represented by a six-vertex induced symmetry graph generated by selected half-turn and quarter-turn rotations.

Another limitation is that the commutation relation alone does not capture the full algebraic structure of a Lie group. Distinct Lie groups may generate isomorphic symmetry graphs while differing substantially in their Lie algebras, structure constants, representation theory, or topology. In particular, the symmetry graph does not distinguish between local and global properties of Lie groups; groups sharing the same commutation structure may nevertheless possess different topological characteristics. Thus, the symmetry graph should be viewed as a combinatorial projection of the symmetry structure rather than a complete invariant of the group.

Moreover, for continuous groups, the number and nature of monochromatic subgraphs may depend on the particular finite subset of operators chosen for analysis. Therefore, while the Ramsey framework remains applicable to continuous symmetry groups, it is most naturally interpreted as a tool for extracting and analyzing finite commutation patterns embedded within richer infinite algebraic structures.

7. Conclusions

A Ramsey-theoretic approach to symmetry was developed. Symmetry operations were represented as vertices of complete bi-colored graphs, called symmetry graphs (SGs), in which commuting operators were connected by maroon edges and non-commuting operators by teal edges.

The introduced construction transforms the commutation structure of symmetry groups into combinatorial objects suitable for Ramsey-theoretic analysis. The coloring of the symmetry graph is induced by the algebraic structure of the symmetry group and is invariant under similarity transformations of the representation space.

The developed framework demonstrates that sufficiently rich symmetry groups inevitably contain monochromatic commuting or non-commuting substructures. In particular, every six-vertex symmetry graph necessarily contains a monochromatic triangle as a consequence of the classical Ramsey theorem $R(3,3) = 6$.

The proposed framework was illustrated for the equilateral triangle, tetrahedral symmetry group, crystallographic point groups, infinite Cairo tilings, the triangular Ising ferromagnet, and motion of the particle in the central potential. These examples demonstrate that symmetry graphs arise naturally in geometry, crystallography, tiling theory, and statistical physics.

The introduced symmetry graphs reveal both Abelian and non-Abelian sectors of symmetry groups. Maroon monochromatic subgraphs correspond to mutually compatible symmetry operations, whereas teal monochromatic subgraphs correspond to intrinsically non-commuting operator structures.

https://doi.org/10.3390/sym18061041

The framework was further extended to infinite symmetry groups using the infinite Ramsey theorem and to Lie-algebraic structures through the Jacobi identity. These results demonstrate that symmetry graphs possess both combinatorial and higher-order algebraic organization.

The present work establishes a new connection between symmetry theory, Ramsey theory, graph theory, and operator algebra. The suggested approach may provide a new combinatorial language for the study of symmetry structures in mathematics and physics.

One-dimensional symmetries give rise to semi-transitive, complete bi-colored graphs for which $R_{semi-trans}(3,3) = 5$, in contrast to non-transitive graphs for which $R(3,3) = 6$.

Funding: This research received no external funding.

Data Availability Statement: The original contributions presented in this study are included in the article. Further inquiries can be directed to the corresponding author.

Acknowledgments: The author is thankful to Yelena Bormashenko for her kind help in preparing this paper. The author is indebted to anonymous reviewers for their fruitful review of the paper.

Conflicts of Interest: The author declares no conflicts of interest.

Abbreviations

The following abbreviations are used in this manuscript:

SG Symmetry Graph
1D One-dimensional

Appendix A. Commutation Rules for the Symmetry Operations Inherent for Tetrahedron

Pair of Operators	Commutation Rule	Edge Color
$\hat{e}, \hat{r}$	Commute	Maroon
$\hat{e},\ \hat{r}^2$	Commute	Maroon
$\hat{e}, \hat{\sigma}_1$	Commute	Maroon
$\hat{e}, \hat{\sigma}_2$	Commute	Maroon
$\hat{e}, \hat{\bar{R}}$	Commute	Maroon
$\hat{r},\ \hat{r}^2$	Commute	Maroon
$\hat{r},\ \hat{\sigma}_1$	Do not commute	Teal
$\hat{r},\ \hat{\sigma}_2$	Do not commute	Teal
$\hat{r},\ \hat{\bar{R}}$	Commute	Maroon
$\hat{r}^2, \hat{\sigma}_1$	Do not commute	Teal
$\hat{r}^2, \hat{\sigma}_2$	Do not commute	Teal
$\hat{r}^2, \hat{\bar{R}}$	Commute	Maroon
$\hat{\sigma}_1, \hat{\sigma}_2$	Do not commute	Teal
$\hat{\sigma}_1, \hat{\bar{R}}$	Do not commute	Teal
$\hat{\sigma}_2, \hat{\bar{R}}$	Do not commute	Teal

Appendix B. Commutation Rules for the Symmetry Operations Inherent for the Cairo Tiling

Pair of Operators	Commutation Rule	Edge Color
$\hat{T}_{\vec{v}}, \hat{T}_{\vec{w}}$	Always commute	Maroon
$\hat{T}_{\vec{v}}, \hat{R}_{P,\theta}$	Commute only if $\hat{Q}_\theta \vec{v} = \vec{v}$	Maroon, teal
$\hat{T}_{\vec{v}}, \hat{M}_l$	Commute if $\vec{v} \parallel \ell$	Maroon, teal
$\hat{T}_{\vec{v}}, \hat{G}_{l,\vec{u}}$	Commute if $\vec{v} \parallel \ell$	Maroon, teal
$\hat{R}_{P,\theta}, \hat{R}_{P,\phi}$	Same center: commute	Maroon
$\hat{R}_{P,\theta}, \hat{R}_{Q,\phi}$	Different centers: generally, do not commute	Teal, maroon
$\hat{R}_{P,\theta}, \hat{M}_l$	Commute only in special cases	Teal, maroon
$\hat{M}_{l_1}, \hat{M}_{l_2}$	Commute if $\ell_1 = \ell_2$ *or* $\ell_1 \perp \ell_2$	Maroon, teal
$\hat{G}_{l,\vec{u}}, \hat{M}_l$	Do not commute for true glide, $\vec{u} \neq 0$.	Teal, maroon
$\hat{G}_{l,\vec{u}_1}, \hat{G}_{l,\vec{u}_2}$,	Commute only in special lattice-compatible cases	Teal, maroon

Appendix C. Non-Commutation of Reflections for 1D Symmetries

Let us demonstrate non-commutation of 1D reflections A short calculation gives:

$$\hat{S}_p \hat{S}_q(x) = x + 2(p - q), \tag{A1}$$

whereas:

$$\hat{S}_q \hat{S}_p(x) = x + 2(q - p). \tag{A2}$$

Hence:

$$\hat{S}_p \hat{S}_q = \hat{T}_{2(p-q)}, \tag{A3}$$

$$\hat{S}_q \hat{S}_p = \hat{T}_{-2(p-q)}, \tag{A4}$$

which coincide only when $p = q$. Therefore, $\left[\hat{S}_p, \hat{S}_q\right] \neq 0 (p \neq q)$.

Appendix D. Analysis of Symmetry of Quadrangle, Illustrating the Jacobi Identity

Consider the symmetry of the quadrangle. We address three symmetries of the quadrangle, namely, $\hat{S}_1 = \hat{r}_\pi$, $\hat{S}_2 = \hat{r}_{\pi/2}$, $\hat{S}_3 = \hat{\sigma}_x$, where $\hat{S}_1$ and $\hat{S}_2$ are rotations by π and $\frac{\pi}{2}$ about the center of the quadrangle, and $\hat{S}_3$ is the x-reflection, thus $\mathfrak{H} = \{\hat{r}_\pi, \hat{r}_{\pi/2}, \hat{\sigma}_x\}$. Here, in the matrix representation:

$$\hat{r}_\pi = \begin{pmatrix} -1 & 0 \\ 0 & -1 \end{pmatrix}, \hat{r}_{\pi/2} = \begin{pmatrix} 0 & -1 \\ 1 & 0 \end{pmatrix}, \hat{\sigma}_x = \begin{pmatrix} 1 & 0 \\ 0 & -1 \end{pmatrix}. \tag{A5}$$

Then:

$$\left[\hat{S}_1, \hat{S}_2\right] = 0, \left[\hat{S}_1, \hat{S}_3\right] = 0, \tag{A6}$$

https://doi.org/10.3390/sym18061041

Because $\hat{S}_1 = \hat{r}_\pi = -\hat{e}$ is central. But

$$[\hat{S}_2, \hat{S}_3] \neq 0. \tag{A7}$$

Indeed, $[\hat{S}_2, \hat{S}_3] = \hat{r}_{\pi/2}\hat{\sigma}_x - \hat{\sigma}_x\hat{r}_{\pi/2} = \begin{pmatrix} 0 & 2 \\ 2 & 0 \end{pmatrix} = 2\hat{\sigma}_d$, where $\hat{\sigma}_d = \begin{pmatrix} 0 & 1 \\ 1 & 0 \end{pmatrix}$ is the reflection in the diagonal $y = x$.

Now, the important point: $[\hat{S}_2, \hat{S}_3] = 2\hat{\sigma}_d \notin \mathfrak{H}$, because $\mathfrak{H} = \{\hat{S}_1, \hat{S}_2, \hat{S}_3\} = \{\hat{r}_\pi, \hat{r}_{\pi/2}, \hat{\sigma}_x\}$. Thus, $\mathfrak{H}$ is not commutation-closed. Nevertheless, Jacobi gives: $[\hat{S}_1, [\hat{S}_2, \hat{S}_3]] = 0$. Indeed, $[\hat{S}_1, [\hat{S}_2, \hat{S}_3]] = -[\hat{e}, 2\hat{\sigma}_d] = 0$. So, this is exactly the case when $[\hat{S}_1, \hat{S}_2] = [\hat{S}_1, \hat{S}_3] = 0$, $[\hat{S}_2, \hat{S}_3] \neq 0$, but $[\hat{S}_2, \hat{S}_3] \notin \mathfrak{H}$. Therefore, Jacobi identity produces the nontrivial constraint $[\hat{S}_1, [\hat{S}_2, \hat{S}_3]] = 0$. This example genuinely emerges from the symmetry group of a shape, namely, the square.

References

1. Van der Waerden, B.L. *Algebra*; Springer: Berlin, Germany, 1967.
2. Armstrong, M.A. *Groups and Symmetry*; Springer: New York, NY, USA, 1988. [CrossRef]
3. Artin, M. *Algebra*; Prentice Hall: Upper Saddle River, NJ, USA, 1991.
4. Steinberg, B. *Representation Theory of Finite Groups: An Introductory Approach*; Springer: New York, NY, USA, 2012. [CrossRef]
5. Serre, J.-P. *Linear Representations of Finite Groups*; Springer: New York, NY, USA, 1977.
6. Wigner, E.P. Violations of Symmetry in Physics. In *Philosophical Reflections and Syntheses*; Mehra, J., Ed.; The Collected Works of Eugene Paul Wigner; Springer: Berlin/Heidelberg, Germany, 1995; Volume B/6.
7. Bradley, C.J.; Cracknell, A.P. *The Mathematical Theory of Symmetry in Solids*; Oxford University Press: Oxford, UK, 1972.
8. Tinkham, M. *Group Theory and Quantum Mechanics*; McGraw–Hill: New York, NY, USA, 1964.
9. Vincent, A. *Molecular Symmetry and Group Theory*; Wiley: Chichester, UK, 2013.
10. Lax, M. *Symmetry Principles in Solid State and Molecular Physics*; Wiley: New York, NY, USA, 1974.
11. Cornwell, J.F. *Group Theory in Physics*; Academic Press: London, UK, 1984.
12. Bormashenko, E.; Frenkel, M. The Three-Body Problem: The Ramsey Approach and Symmetry Considerations in the Classical and Quantum Field Theories. *Symmetry* **2025**, *17*, 1404. [CrossRef]
13. Georgi, H. *Lie Algebras in Particle Physics*; Westview Press: Boulder, CO, USA, 1999. [CrossRef]
14. Griffiths, D.J.; Schroeter, D.F. *Introduction to Quantum Mechanics*, 3rd ed.; Cambridge University Press: Cambridge, UK, 2018. [CrossRef]
15. Shankar, R. *Principles of Quantum Mechanics*, 2nd ed.; Springer: New York, NY, USA, 2012. [CrossRef] [PubMed]
16. Humphreys, J.E. *Introduction to Lie Algebras and Representation Theory*; Springer: New York, NY, USA, 1972.
17. Weyl, H. *The Theory of Groups and Quantum Mechanics*; Dover Publications: New York, NY, USA, 1950.
18. Hamermesh, M. *Group Theory and Its Application to Physical Problems*; Dover Publications: New York, NY, USA, 1989.
19. Brauer, R.; Fowler, K.A. On groups of even order. *Ann. Math.* **1955**, *62*, 565–583. [CrossRef]
20. Abdollahi, A.; Akbari, S.; Maimani, H.R. Non-commuting graph of a group. *J. Algebra* **2006**, *298*, 468–492. [CrossRef]
21. Iranmanesh, A.; Jafarzadeh, A. On the commuting graph associated with the symmetric and alternating groups. *J. Algebra Appl.* **2008**, *7*, 129–146. [CrossRef]
22. Giudici, M.; Pope, A. On bounding the diameter of the commuting graph of a group. *J. Group Theory* **2014**, *17*, 131–149. [CrossRef]
23. Morgan, G.L.; Parker, C.W. The diameter of the commuting graph of a finite group with trivial centre. *J. Algebra* **2013**, *393*, 41–59. [CrossRef]
24. Solomon, R.M.; Woldar, A.J. Simple groups are characterized by their non-commuting graphs. *J. Group Theory* **2013**, *16*, 793–824. [CrossRef]
25. Cameron, P.J. Graphs defined on groups. *Int. J. Group Theory* **2022**, *11*, 53–107.
26. Graham, R.L.; Rothschild, B.L.; Spencer, J.H. *Ramsey Theory*, 2nd ed.; Wiley: New York, NY, USA, 1990.
27. Jukna, S. *Extremal Combinatorics*, 2nd ed.; Springer: Berlin/Heidelberg, Germany, 2011. [CrossRef]
28. Bollobás, B. *Modern Graph Theory*; Springer: New York, NY, USA, 1998. [CrossRef]
29. West, D.B. *Introduction to Graph Theory*, 2nd ed.; Prentice Hall: Upper Saddle River, NJ, USA, 2001.
30. Diestel, R. *Graph Theory*, 5th ed.; Springer: Heidelberg, Germany, 2017. [CrossRef]
31. Ramsey, F.P. On a Problem of Formal Logic. *Proc. Lond. Math. Soc.* **1930**, *30*, 264–286. [CrossRef]
32. Alon, N.; Spencer, J.H. *The Probabilistic Method*, 4th ed.; Wiley: Hoboken, NJ, USA, 2016.
33. Harris, J.M.; Hirst, J.L.; Mossinghoff, M.J. *Combinatorics and Graph Theory*, 2nd ed.; Springer: New York, NY, USA, 2008. [CrossRef]

34. Todorcevic, S. *Introduction to Ramsey Spaces*; Princeton University Press: Princeton, NJ, USA, 2010.
35. Beineke, L.W.; Wilson, R.J. *Topics in Structural Graph Theory*; Cambridge University Press: Cambridge, UK, 2012.
36. Brualdi, R.A.; Ryser, H.J. *Combinatorial Matrix Theory*; Cambridge University Press: Cambridge, UK, 1991. [CrossRef]
37. Bormashenko, E. Jordan Curves: Ramsey Approach and Topology. *Mathematics* **2026**, *14*, 351. [CrossRef]
38. de Gois, C.; Hansenne, K.; Gühne, O. Uncertainty relations from graph theory. *Phys. Rev. A* **2023**, *107*, 062211. [CrossRef]
39. Xu, Z.-P.; Schwonnek, R.; Winter, A. Bounding the Joint Numerical Range of Pauli Strings by Graph Parameters. *PRX Quantum* **2024**, *5*, 020318. [CrossRef]
40. Gratus, J.; Lambert, C.J.; Robinson, S.J.; Tucker, R.W. Quantum mechanics on graphs. *J. Phys. A Math. Gen.* **1994**, *27*, 6881. [CrossRef]
41. Banakh, T.; Verbitsky, O.; Vorobets, Y. A Ramsey Treatment of Symmetry. *Electron. J. Comb.* **2000**, *7*, R52. [CrossRef] [PubMed]
42. Hall, B.C. *Quantum Theory for Mathematicians*; Springer: New York, NY, USA, 2013. [CrossRef]
43. Bratteli, O.; Robinson, D.W. *Operator Algebras and Quantum Statistical Mechanics*; Springer: Berlin/Heidelberg, Germany, 1987. [CrossRef]
44. Bormashenko, E.; Shvalb, N. Ramsey Approach to Quantum Mechanics. *arXiv* **2024**, arXiv:2411.02082.
45. Akhiezer, N.I.; Glazman, I.M. *Theory of Linear Operators in Hilbert Space*; Nestell, M., Translator; Frederick Ungar Publishing Co.: New York, NY, USA, 1961; Volume I.
46. Gilevich, A.; Shoval, S.; Nosonovsky, M.; Frenkel, M.; Bormashenko, E. Converting Tessellations into Graphs: From Voronoi Tessellations to Complete Graphs. *Mathematics* **2024**, *12*, 2426. [CrossRef]
47. Shi, L.; Xiong, Z.; Wang, H.; Cao, H.; Chen, Z. Quasicrystal approximants in isoreticular metal-organic frameworks via Cairo pentagonal tiling. *Chem* **2024**, *10*, 2464–2472. [CrossRef]
48. Kovács, G.; Nagy, B.; Turgay, N.D. Distance on the Cairo pattern. *Pattern Recognit. Lett.* **2021**, *145*, 141–146. [CrossRef]
49. Bormashenko, E. The Logic of Motion and Rest: A Graph-Theoretical Approach. *Dynamics* **2026**, *6*, 13. [CrossRef]

Disclaimer/Publisher's Note: The statements, opinions and data contained in all publications are solely those of the individual author(s) and contributor(s) and not of MDPI and/or the editor(s). MDPI and/or the editor(s) disclaim responsibility for any injury to people or property resulting from any ideas, methods, instructions or products referred to in the content.